

Verifying Nonlinear Neural Feedback Systems using Polyhedral Enclosures

Samuel I. Akinwande, Chelsea Sidrane, Mykel J. Kochenderfer, Clark Barrett

Abstract—As dynamical systems equipped with neural network controllers (neural feedback systems) become increasingly prevalent, it is critical to develop methods to ensure their safe operation. Verifying safety requires extending control theoretic analysis methods to these systems. Although existing techniques can efficiently handle *linear* neural feedback systems, relatively few scalable methods address the *nonlinear* case. We propose a novel algorithm for forward reachability analysis of nonlinear neural feedback systems. The approach leverages the structure of the nonlinear transition functions of the systems to compute tight polyhedral enclosures (i.e., abstractions). These enclosures, combined with the neural controller, are then encoded as a mixed-integer linear program (MILP). Optimizing this MILP yields a sound over-approximation of the forward-reachable set. We evaluate our algorithm on representative benchmarks and demonstrate an order of magnitude improvement over the current state of the art.

Index Terms—Formal Verification, Nonlinear Systems, Neural Networks, Integer Linear Programming.

I. INTRODUCTION

The success of neural networks in the fields of drone racing [24], autonomous driving [10], and system identification [8] underscores the growing interest in using neural networks as controllers for dynamical systems. We refer to these as *neural feedback systems*, and many of their potential uses are in safety-critical settings. In order to realize this potential, it is crucial to develop verification techniques to ensure their safety. Although there is a rich body of work on verification for classical control systems [4], [7], [41], these techniques are often ill-suited for neural feedback systems due to nonlinearities and the common practice of viewing neural networks as black boxes. To address this gap, recent work has focused on creating methods for the safety verification of neural feedback systems [13], [19], [26], [38], [44], [45]. These methods can be broadly classified into two categories: propagation-based methods and combinatorial methods [11], each offering distinct approaches to analyzing the behavior of neural feedback systems.

Following the terminology of [11], we define *propagation-based methods* as those that systematically propagate an initial set through both the dynamical system and the neural network.

Samuel Akinwande and Mykel Kochenderfer are with the Department of Aeronautical and Astronautical Engineering, Stanford University, Stanford, CA, 94305 USA e-mail:akinwande@cs.stanford.edu

Clark Barrett is with the Department of Computer Science, Stanford University, Stanford, CA, 94305 USA

Chelsea Sidrane is with the Division of Robotics, Perception and Learning, Intelligent Systems Department, School of Electrical Engineering & Computer Science, KTH Royal Institute of Technology, Stockholm, Sweden

These methods often rely on abstractions (e.g., Taylor models [9], [18], Bernstein polynomials [14], zonotopes [37], and polynomial zonotopes [27]) to achieve efficient computations. To address the loss of precision caused by these abstractions, some tools introduce refinement algorithms that can improve the tightness of the analysis [12], [29], [36]. CORA is a prominent tool for verifying neural feedback systems using abstraction propagation [2]. It computes reachable sets by combining approximations of the system dynamics with non-convex network abstractions (e.g., polynomial zonotopes). For the state space, CORA employs conservative linear [3] and polynomial [1] abstractions. To handle the neural network, it uses reachability analysis [25], [27] to compute a non-convex enclosure of the network’s outputs. By leveraging these abstraction-based methods alongside non-convex set representations, CORA trades off precision for computational efficiency making it one of the most competitive tools for formally verifying neural feedback systems. Although other propagation-based tools exist, many either lack support for discrete-time nonlinear neural feedback systems [5] or incorporate CORA’s core algorithm [32].

In contrast, we define *combinatorial methods* as those that prioritize capturing the combinatorial structure of the neural network controller. Tools built on these methods verify properties by solving combinatorial problems. Existing approaches include techniques that model neural feedback systems as hybrid systems [20] or as hybrid zonotopes [39], [45], as well as methods that encode the problem as marching trees [43] or integer linear programs [38]. By emphasizing the combinatorial structure of the neural network controller, these methods trade off computational complexity for precision. A notable example is the OVERTVerify algorithm [38], which computes reachable sets for nonlinear neural feedback systems. OVERTVerify uses the OVERT algorithm and relational overapproximations to construct constraints that implicitly bound multivariate nonlinear functions. While alternative combinatorial tools exist for ReLU networks with nonlinear dynamics (e.g., those employing hybrid zonotopes [39]), OVERTVerify has thus far remained one of the most scalable combinatorial approaches for capturing reachability, due to its ability to efficiently handle larger systems while preserving high precision in its reachability analysis. Combinatorial methods, including OVERTVerify, are often prohibitively expensive computationally, and thus, many successful verification tools instead rely on abstraction propagation and refinement [31].

In this paper, we introduce the OvertPoly algorithm, which aims to address some of the limitations of combinatorial methods. We exploit a structured representation of the neural

feedback system to create a precise combinatorial method with computational performance comparable to propagation-based methods.

While our approach is based on the OVERT algorithm [38], it is also closely related to *subdividable linear efficient function enclosures* (SLEFEs) [33], [35] and *minimum volume simplicial enclosures* (MINVO) [42]. SLEFEs enclosure multivariate polynomials by computing upper and lower bounds using a second difference operator and its corresponding basis. In contrast to SLEFEs, our method generalizes to higher dimensions by composing lower-dimensional enclosures. Furthermore, rather than using simplices, as in MINVO enclosures, our approach makes use of more general polyhedra to bound functions. Finally, our method can be applied to a broader class of functions than those handled by either SLEFEs or MINVO enclosures.

Our contributions include the following:

- We introduce a novel algorithm for computing tight polyhedral enclosures for multivariate nonlinear functions. This algorithm combines decomposition with optimization-based bounding algorithms to provide arbitrarily tight bounds on nonlinear functions.
- We provide an efficient method for encoding polyhedral enclosures as mixed integer linear programs (MILPs). Our encoding addresses the limitations of existing approaches by exploiting problem structure to help minimize the encoding size.
- We define concrete and symbolic reachability algorithms. We use a dependency graph framework to represent systems of MILPs and to optimize the encoding.
- We implement and evaluate our algorithm and show that it performs better than both OVERTVerify and CORA on a set of neural feedback system benchmarks.

The rest of the paper is organized as follows. Section II covers background material, Section III defines the problem of neural feedback system verification, and Section IV discusses the theory of Polyhedral enclosures. Then, in Section V, we introduce our OvertPoly algorithm and discuss its implementation. Section VII reports on our experimental evaluation, and Section VIII concludes.

II. BACKGROUND

A. Notation

We denote the set of integers as \mathbb{Z} , the set of natural numbers (integers greater than zero) as \mathbb{N} , the set of real numbers as \mathbb{R} , and the set of non-negative real numbers as \mathbb{R}_+ . If \mathcal{X} is a set, we denote the *power set* of \mathcal{X} (i.e., the set of all subsets of \mathcal{X}) as $2^{\mathcal{X}}$. We use $[i..j]$ to represent the set $\{z \in \mathbb{Z} \mid i \leq z \leq j\}$, $[i, j]$ to represent the set $\{r \in \mathbb{R} \mid i \leq r \leq j\}$, and $[n]$ to abbreviate $[1..n]$.

If S is any finite *sequence* (s_1, \dots, s_n) , we write $|S|$ to denote n , the length of the sequence, and S_i to denote the i^{th} element of the sequence. We write $S_{[i..j]}$ for the sequence (s_i, \dots, s_j) and $S \circ S'$ for the sequence obtained by appending the sequence S' to the end of S . If a sequence is used where a set is expected, the meaning is the set of elements in the sequence (e.g., $s \in S$ means that s occurs in the sequence S).

We use the same notation for both vectors and sequences and treat them as interchangeable.

We use \preceq and \succeq to describe element-wise inequalities for finite sequences, defined as follows. If x and y are sequences of size n , then $x \preceq y$ is also a sequence of size n , with $(x \preceq y)_i = 1$, if $x_i \leq y_i$, and 0 otherwise. We define $x \succeq y$ similarly. We write $x \cdot y$ for the dot product (i.e. sum of element-wise products) of vectors x and y . We write $\vec{0}$ for the zero vector, $\vec{1}$ for the vector of all ones, and e_i for the i^{th} unit vector. The sizes of these vectors will be left implicit when it is clear from context. A *convex combination vector* is a vector whose entries are non-negative and sum to 1. We adopt the convention that such vectors are called θ and write the convex combination vector conditions as $\theta \cdot \vec{1} = 1$ and $\theta \succeq \vec{0} = \vec{1}$. For a function $f : \mathcal{X} \rightarrow \mathbb{R}$ and a set $\mathcal{X}' \subseteq \mathcal{X}$, we define the *image* of \mathcal{X}' under f as $f(\mathcal{X}') := \{f(\vec{x}) \mid \vec{x} \in \mathcal{X}'\}$. Similarly, if S is a sequence, then $f(S)$ is the sequence $(f(S_1), f(S_2), \dots)$. For $\mathcal{X}' \subseteq \mathcal{X}$, we define the *restriction* of f to \mathcal{X}' as the function $f^{\mathcal{X}'} : \mathcal{X}' \rightarrow \mathbb{R}$ such that $f^{\mathcal{X}'}(x) = f(\vec{x})$ for every $x \in \mathcal{X}'$.

B. Polyhedra

Let P be a set of $k+1$ points: $P = \{p_0, \dots, p_k\}$, with each $p_i \in \mathbb{R}^n$. The *convex hull* of P is

$$\mathbf{conv}(P) = \{\theta_0 p_0 + \dots + \theta_k p_k \mid \theta \cdot \vec{1} = 1, \theta \succeq \vec{0} = \vec{1}\}. \quad (1)$$

The points in P are *affinely independent* iff the set $\{p_1 - p_0, \dots, p_k - p_0\}$ is linearly independent. The *polyhedron formed* by a set of points P is just $\mathbf{conv}(P)$. A subset of \mathbb{R}^n is a polyhedron if it is the convex hull of a finite set of points in \mathbb{R}^n .¹

Definition 1 (*k-Simplex*). A *polyhedron* \mathcal{S} is a *k-simplex* if it is the convex hull of $k+1$ affinely independent points. A *polyhedron* is a *simplex* if it is a *k-simplex* for some k , and k is called its *dimension*.

If \mathcal{S} is a *k-simplex*, let $\mathbf{vert}(\mathcal{S})$, the *vertices* of \mathcal{S} , denote the (unique) set of $k+1$ points P such that $\mathcal{S} = \mathbf{conv}(P)$. A *face* of \mathcal{S} is the convex hull of any non-empty subset of $\mathbf{vert}(\mathcal{S})$. A face of \mathcal{S} is *maximal* if it is the convex hull of k points in $\mathbf{vert}(\mathcal{S})$.

Definition 2 (*Simplicial k-Complex*). A *simplicial complex* Δ is a set of simplices such that:

- Every face of a simplex in Δ is also in Δ
- Every non-empty intersection of two simplices $\mathcal{S}_1, \mathcal{S}_2 \in \Delta$ is a face of both \mathcal{S}_1 and \mathcal{S}_2

Δ is a *pure simplicial k-complex* if the largest dimension of any simplex in Δ is k and if every simplex in Δ of dimension less than k is a face of some simplex in Δ of dimension k .

Definition 3 (*Full-Dimensional*). Let P be a finite set of points in \mathbb{R}^n . We say that P is *full-dimensional* if its affine hull is of dimension n (i.e., the points span the full n -dimensional space).

¹Sometimes the term “polyhedron” is reserved for three-dimensional objects, with the generalization to arbitrary dimensions called a “polytope.” Following [6], [46], we use “polyhedron” also for the general case.

Definition 4 (Point Set Triangulation). *If P is a finite, full-dimensional set of points in \mathbb{R}^n , then a pure simplicial n -complex Δ is a triangulation of P if $P = \bigcup_{S \in \Delta} \text{vert}(S)$ and $\text{conv}(P) = \bigcup_{S \in \Delta} S$.*

Let P be a finite, full-dimensional set of points in \mathbb{R}^n . Let C be a closed n -ball. We use C^O to denote the corresponding open n -ball and C^S to denote the hypersphere that forms the surface of C . The vertices—with respect to P —of C are defined as $V_P(C) = C \cap P$. Now, let Δ be a triangulation of P , and let S be an n -simplex in Δ . We define $C(S)$ to be the n -ball whose boundary is the smallest hypersphere that circumscribes S (i.e., $C(S)$ is the smallest closed n -ball C such that $S \subseteq C$ and $C^O \cap \text{vert}(S) = \emptyset$). S satisfies the *Delaunay condition* and is called a *Delaunay simplex of P* if $V_P(C(S)^O) = \emptyset$ (i.e., the only points from P contained in $C(S)$ are on its surface). Δ is a *Delaunay triangulation* if every n -simplex in Δ satisfies the Delaunay condition. P has a Delaunay triangulation iff it is full-dimensional.

For a point $\vec{x} \in \text{conv}(P)$, let $S_\Delta(\vec{x})$ be the n -simplex in Δ containing \vec{x} , and let $\theta_\Delta(\vec{x})$ be the convex combination vector such that $\vec{x} = \theta(\vec{x}) \cdot \text{vert}(S_\Delta(\vec{x}))$.

C. Bounding Convex Functions

To compute tight upper and lower bounds for nonlinear one-dimensional functions, we use a method introduced in the OVERT algorithm [38]. For a function $f(\vec{x})$ that is convex on the interval (a, b) , an upper bound can be constructed by symbolically partitioning (a, b) into $m - 1$, ($m > 0$) subintervals with endpoints $(s_0 = a, s_1, \dots, s_{m-1}, s_m = b)$ and defining secant lines from $(s_{i-1}, f(s_{i-1}))$ to $(s_i, f(s_i))$ for $i \in [m]$. The point locations s_i are then optimized to minimize the area between the secant lines and the function $f(\vec{x})$. A lower bound can be constructed similarly by partitioning (a, b) into subintervals with endpoints s_i , $i \in [0..m]$ and defining a sequence of line segments from (s_i, t_i) to (s_{i+1}, t_{i+1}) , $i \in [0..m - 1]$ in such a way that $t_0 = f(a)$, $t_m = f(b)$, each segment from (s_i, t_i) to (s_{i+1}, t_{i+1}) , $i \in [m - 2]$ is tangent to $f(\vec{x})$, and the area between the line segments and the function is once again minimized. Bounds for a univariate function $f(\vec{x})$ that is concave over an interval are computed analogously, using a series of secants for lower bounds and a series of tangents for upper bounds. The tightness of the bounds can be adjusted by modifying the parameter m . Bounds over an arbitrary interval can be computed by first decomposing the function into intervals of uniform convexity and then composing the bounds obtained for each region (see Section IV-A). Details of these methods can be found in [38].

D. ReLU Functions as Mixed Integer Constraints

A *feed-forward neural network* (FNN) is a function constructed by composing linear and nonlinear operations. These operations are organized in *layers*, where each layer applies a linear transformation and (optionally) a nonlinear operation. The elements within a layer are referred to as *neurons*, and the nonlinear operations are known as *activation functions*. In this work, we focus on the Rectified Linear Unit (ReLU) activation

function, defined as $\text{ReLU}(x) = \max(x, 0)$. We refer to FNNs using only this activation function as *ReLU-activated feed-forward neural networks*.

ReLU activated FNNs specify piecewise-linear functions and can therefore be formulated as mixed-integer linear programs (MILPs). Following the technique used by the MIPVerify algorithm [40], we encode ReLU constraints as follows. Let $l, u \in \mathbb{R}$ be real numbers intended to bound x , with $l \leq 0 \leq u$,² and let $\mathbb{1}_{(x \geq 0)}$ be an indicator variable. Then both the ReLU function $y = \max(x, 0)$ and the bounds $l \leq x \leq u$ can be represented by the constraints

$$y \leq x - l(1 - \mathbb{1}_{(x \geq 0)}), \quad y \geq x, \quad y \leq u \cdot \mathbb{1}_{(x \geq 0)}, \quad y \geq 0. \quad (2)$$

To encode a ReLU-activated FNN, the linear layers are expressed as standard linear constraints, while the nonlinear ReLU constraints use Equation (2).

III. NEURAL FEEDBACK SYSTEMS

We define a discrete-time neural feedback system \mathcal{D} as a tuple $\langle n, I, F, E, u, \delta, T, G, A \rangle$, where $n \in \mathbb{N}$ is the *dimension* of the system (i.e., every state of the system is an element of \mathbb{R}^n), $I \subseteq \mathbb{R}^n$ is the set of *initial states*, F is a sequence (f_1, \dots, f_n) of *state update functions* with $f_i : \mathbb{R}^n \rightarrow \mathbb{R}$, $E \subseteq \mathbb{R}^n$ is a *perturbation error set* (i.e., a set from which an error term may be introduced when computing the next state), $u : \mathbb{R}^n \rightarrow \mathbb{R}^n$ is the *control function*, $\delta \in \mathbb{R}_+$ is the *time step size*, $T \in \mathbb{N}$ is the *number of time steps*, $G \subseteq \mathbb{R}^n$ is the set of *goal states*, and $A : [0..T] \rightarrow 2^{\mathbb{R}^n}$ is a function from time steps to the set of *avoid states* (i.e., unsafe states) at that time step.

States evolve over a sequence of T discrete time steps, each of duration δ , and the *time horizon* is $\delta \cdot T$. If $\vec{x} \in \mathbb{R}^n$ is a system state, the next-state function $\text{next}^{\mathcal{D}} : \mathbb{R}^n \rightarrow 2^{\mathbb{R}^n}$ defines the set of possible next states (it is a set because of the nondeterminism introduced by the error term) as follows. For each $i \in [1..n]$,

$$\text{next}^{\mathcal{D}}(\vec{x})_i = \{ \vec{x}_i + (f_i(\vec{x}) + u(\vec{x})_i + \epsilon) \cdot \delta \mid \epsilon \in E \} \quad (3)$$

Note that f_i and u may depend on the entire previous state \vec{x} , not just on \vec{x}_i .

We assume that each f_i is from the class of Lipschitz continuous multivariate functions composed of rational operations (i.e., $+$, $-$, \times , \div) on univariate elementary functions.³ We call these functions *extended rational nonlinear functions*.⁴ We also assume that the neural network controller u is a multilayer perceptron with n inputs, n outputs, and ReLU activations.

A trajectory $\tau^{\mathcal{D}}(\mathcal{X}_0)$, where $\mathcal{X}_0 \subseteq I$, is defined as the sequence of sets of states $(\mathcal{X}_0, \mathcal{X}_1, \dots, \mathcal{X}_T)$, where $\mathcal{X}_i = \text{next}^{\mathcal{D}}(\mathcal{X}_{i-1})$ for $i \in [1..T]$.

²Note that in the case that $l \leq u < 0$ or $0 < l \leq u$, a much simpler linear encoding is possible.

³Following the convention of [34], we define elementary functions as the trigonometric functions, their inverses, the exponential functions, and logarithmic functions.

⁴While we only consider a subset of nonlinear functions, the Kolmogorov-Arnold representation theorem [28] suggests that our approach can be generalized to arbitrary nonlinear functions.

A system \mathcal{D} is *safe* if it satisfies the following reach-avoid properties:

$$\forall \vec{x}_0 \in I. \exists t \in [0..T]. \tau^{\mathcal{D}}(\{\vec{x}_0\})_t \subseteq G, \quad (4)$$

$$\forall t \in [0..T]. \tau^{\mathcal{D}}(I)_t \cap A(t) = \emptyset. \quad (5)$$

Property 4 is a *reach* property. It states that every trajectory starting from some state in the initial state set reaches the goal set (specified by G) within the specified time horizon. On the other hand, Property 5 is an *avoid* property, requiring that the system avoids any unsafe states (A) at each time within the given time horizon.

A. Running Example: Unicycle Car Model

As a running example, we use a discrete-time version of the unicycle car model example from the 2023 ARCH competition [31]. The car is modeled with four variables, representing the x and y coordinates in a plane, the steering angle, and the velocity magnitude. Formally, we define $\mathcal{U} = \langle n^{\mathcal{U}}, I^{\mathcal{U}}, F^{\mathcal{U}}, E^{\mathcal{U}}, u^{\mathcal{U}}, \delta^{\mathcal{U}}, T^{\mathcal{U}}, G^{\mathcal{U}}, A^{\mathcal{U}} \rangle$, where $n^{\mathcal{U}} = 4$, $I^{\mathcal{U}} = [9.5, 9.55] \times [-4.5, -4.45] \times [2.1, 2.11] \times [1.5, 1.51]$, $F^{\mathcal{U}}(\vec{x}) = (\vec{x}_4 \cos(\vec{x}_3), \vec{x}_4 \sin(\vec{x}_3), 0, 0)$, $E = \{0\} \times \{0\} \times \{0\} \times [-10^{-4}, 10^{-4}]$, $u^{\mathcal{U}}$ is computed by a neural network with one hidden layer with 500 neurons and four outputs, the first two of which are set to the constant zero value (i.e., the controller only affects the velocity and steering), $\delta^{\mathcal{U}} = 0.2$, $T^{\mathcal{U}} = 50$, $G^{\mathcal{U}} = [-0.6, 0.6] \times [-0.2, 0.2] \times [-0.06, 0.06] \times [-0.3, 0.3]$, and $A^{\mathcal{U}}(t) = \emptyset$ for every $t \in [0..T^{\mathcal{U}}]$. At each step, the system updates its x and y coordinates based on the steering and velocity control outputs, where the velocity output is subject to a small amount of perturbation. It must reach a goal position near the origin with a steering angle near 0 and with a low velocity. Formally, we would like to verify that Equation (4) holds for \mathcal{U} .

IV. POLYHEDRAL ENCLOSURES

In our verification approach, we use *polyhedral enclosures* to provide tight overapproximations of nonlinear functions. In this section, we provide a formal definition of a polyhedral enclosure and then discuss how to construct and compose them.

Definition 5 (Bounding Set). A bounding set is a tuple $\mathcal{B} = \langle n, P, L, U \rangle$, where $n \in \mathbb{N}$, P is a finite, full-dimensional set of points in \mathbb{R}^n , and L and U are functions from P to \mathbb{R} , such that $L(\vec{p}) \leq U(\vec{p})$ for all $\vec{p} \in P$. The domain of \mathcal{B} is defined as $\text{dom}(\mathcal{B}) = \text{conv}(P)$.

Example 1. Let $\vec{p}_1 = (-5, -5)$, $\vec{p}_2 = (-5, 5)$, $\vec{p}_3 = (5, -5)$, $\vec{p}_4 = (5, 5)$ be points in \mathbb{R}^2 and let $P_1 = \{\vec{p}_1, \vec{p}_2, \vec{p}_3, \vec{p}_4\}$. Then, let \mathcal{B}^1 be the bounding set $\langle 2, P_1, L_1, U_1 \rangle$, with $U_1(\vec{p}) = 5$ and $L_1(\vec{p}) = -5$ for every $\vec{p} \in P_1$. The domain of \mathcal{B}^1 , $\text{dom}(\mathcal{B}^1)$, is a square with sides of length 10 centered at the origin.

Definition 6 (Polyhedron formed by Bounding Set). Let $\mathcal{B} = \langle n, P, L, U \rangle$ be a bounding set. We define the vertices of the bounding set as:

$$V(\mathcal{B}) := \{(\vec{p}, L(\vec{p})) : \vec{p} \in P\} \cup \{(\vec{p}, U(\vec{p})) : \vec{p} \in P\}.$$

We define the $(n + 1\text{-dimensional})$ polyhedron formed by \mathcal{B} as

$$\mathcal{P}(\mathcal{B}) := \text{conv}(V(\mathcal{B})).$$

The polyhedron formed by \mathcal{B}^1 from Example 1 is a cube with sides of length 10 centered at the origin.

Definition 7 (Polyhedral Enclosure). Let $\mathcal{B} = \langle n, P, L, U \rangle$ be a bounding set, let Δ be a Delaunay point set triangulation of P , and let Δ_n be the set of all n -simplices in Δ . We then define the bounding set associated with a simplex $S \in \Delta_n$ as:

$$\mathcal{B}_S := \langle n, \text{vert}(S), L^{\text{vert}(S)}, U^{\text{vert}(S)} \rangle,$$

We define the polyhedral enclosure formed by \mathcal{B} and Δ as:

$$\mathcal{E}(\mathcal{B}, \Delta) := \bigcup_{S \in \Delta_n} \mathcal{P}(\mathcal{B}_S).$$

Example 2. Consider again the bounding set \mathcal{B}_1 from Example 1. Let Δ_1 be the triangulation of P_1 whose 2-simplices are the triangles T_1 , with vertices $\vec{p}_1, \vec{p}_2, \vec{p}_3$, and T_2 , with vertices $\vec{p}_2, \vec{p}_3, \vec{p}_4$. Then, $\mathcal{P}(\mathcal{B}_{T_1}^1)$ and $\mathcal{P}(\mathcal{B}_{T_2}^1)$ are the two prisms obtained by slicing the polyhedron formed by \mathcal{B}^1 in half along the plane $x_1 + x_2 = 0$. And $\mathcal{E}(\mathcal{B}^1, \Delta_1)$ is their union, which, in this case, is again just the polyhedron formed by \mathcal{B}^1 .

Definition 8 (Function Enclosure). Let $\mathcal{B} = \langle n, P, L, U \rangle$ be a bounding set. A function $f : D \rightarrow \mathbb{R}$, where $\text{dom}(\mathcal{B}) \subseteq D \subseteq \mathbb{R}^n$, is enclosed by \mathcal{B} if for every $\vec{x} \in \text{dom}(\mathcal{B})$ and every Delaunay triangulation Δ of P , $(\vec{x}, f(\vec{x})) \in \mathcal{E}(\mathcal{B}, \Delta)$.

Example 3. Let $f(x_1, x_2) = x_2 \cos(x_1)$. The maximum value of f on $\text{dom}(\mathcal{B}^1)$ is 5 and the minimum value is -5. $\mathcal{E}(\mathcal{B}^1, \Delta)$ is the origin-centered cube with side length 10 for every Delaunay point set triangulation Δ of P_1 . Thus, \mathcal{B}^1 encloses f .

A. Polyhedral Enclosures of Univariate Functions

Let $f : \mathbb{R} \rightarrow \mathbb{R}$ be a function that is twice differentiable on the interval $[a, b]$. We construct a bounding set enclosing f as follows.

We partition the interval into m subintervals of uniform convexity by identifying all points in $[a, b]$ where the second derivative of f vanishes:

$$z_0 := a, \quad z_m := b, \quad \text{and} \quad \frac{d^2}{dx^2} f(z_i) = 0 \text{ for } i = 1, \dots, m-1.$$

Note that if $\frac{d^2}{dx^2} f(\vec{x}) = 0$ for all $x \in [a, b]$, then we set $m = 1$. For each subinterval $[z_i, z_{i+1}]$, we follow the technique described in Section II-C to compute piecewise-linear upper and lower bounds for f on that interval. Stitching all of them together, we get piecewise-linear functions L and U such that $\forall x. a \leq x \leq b \implies L(x) \leq f(x) \leq U(x)$.

Now, we define the point set P to be the set of all endpoints of line segments in the piecewise-linear functions L and U on the interval $[a, b]$ (including a and b themselves). A bounding set enclosing f is then:

$$\mathcal{B} := \langle 1, P, L^P, U^P \rangle$$

B. Composing Polyhedral Enclosures

In this section, we introduce a notion of *composition* for bounding sets. Our goal is to show that composition preserves enclosure.

We start by defining *lifting* and *interpolation*, two operations on bounding sets that are needed to define composition. *Lifting* extends a function to a higher dimensional domain in such a way that the restriction to the original domain is the original function. Lifting is parameterized by a set S , which identifies the indices of the arguments in the higher-dimensional function that correspond to arguments in the original unlifted function (the rest of the higher-dimensional arguments are ignored).

Definition 9 (Lifted Function). *Let $f : \mathbb{R}^k \rightarrow \mathbb{R}$ be a function, let $n > k$, and let $S = \{j_1, \dots, j_k\}$ be a subset of $[1..n]$ of size k with $j_i < j_{i+1}$ for each $i \in [1..k-1]$. We define f lifted to n by S , $f \uparrow^{S,n}$ as follows. For each $\vec{y} \in \mathbb{R}^n$, $(f \uparrow^{S,n})(\vec{y}) = f(\vec{x})$, where $\vec{x} \in \mathbb{R}^k$ and for each $i \in [1..k]$, $x_i = y_{j_i}$.*

Example 4. *Let f be the function from Example 3, and let $S = \{3, 4\}$. Then, if $\vec{y} = (y_1, y_2, y_3, y_4)$, $f \uparrow^{S,4}(y) = y_4 \cos(y_3)$.*

Definition 10 (Lifted Bounding Set). *Let $\mathcal{B} := \langle k, P, L, U \rangle$ be a bounding set, let $n > k$, let $S = \{j_1, \dots, j_k\}$ be a subset of $[1..n]$ of size k with $j_i < j_{i+1}$ for each $i \in [1..k-1]$, and let $\vec{p}^l, \vec{p}^u \in \mathbb{R}^n$, with $\vec{p}_i^l < \vec{p}_i^u$ for $i \in [1..n] \setminus S$. We define \mathcal{B} lifted to n by S from \vec{p}^l to \vec{p}^u , $\mathcal{B} \uparrow_{\vec{p}^l, \vec{p}^u}^{S,n}$ as follows. $\mathcal{B} \uparrow_{\vec{p}^l, \vec{p}^u}^{S,n} = \langle n, P', L \uparrow^{S,n}, U \uparrow^{S,n} \rangle$, where $P' = \{\vec{p}' \in \mathbb{R}^n \mid \exists \vec{p} \in P. \vec{p}'_i = \vec{p}_i \text{ if } i \in S \text{ and } \vec{p}'_i \in \{\vec{p}_i^l, \vec{p}_i^u\} \text{ otherwise.}\}$*

Note that the purpose of \vec{p}^l and \vec{p}^u is to provide lower and upper bounds for the new dimensions added when lifting the points in P , to ensure that P' is full-dimensional.

Example 5. *Let \mathcal{B}^1 be the bounding set from Example 1, let $S = \{1, 2\}$, let $\vec{p}^u = (0, 0, 5)$, and let $\vec{p}^l = (0, 0, -5)$. Then, $\mathcal{B} \uparrow_{\vec{p}^l, \vec{p}^u}^{S,3}$ is a bounding set whose domain is the cube with sides of length 10 centered at the origin, and the polyhedron formed by the lifted bounding set is a hypercube in \mathbb{R}^4 also centered at the origin.*

Theorem 1. *If a bounding set $\mathcal{B} = \langle k, P, L, U \rangle$ encloses a function f , then for every $n > k$, $S \subset [1..n]$ with $|S| = k$, and $\vec{p}^l, \vec{p}^u \in \mathbb{R}^n$, with $\vec{p}_i^l < \vec{p}_i^u$ for $i \in [1..n] \setminus S$, $\mathcal{B} \uparrow_{\vec{p}^l, \vec{p}^u}^{S,n}$ encloses $f \uparrow^{S,n}$.*

Proof. Let $\mathcal{B} \uparrow_{\vec{p}^l, \vec{p}^u}^{S,n} = \langle n, P', L \uparrow^{S,n}, U \uparrow^{S,n} \rangle$, and let \vec{y} be a point in $\text{dom}(\mathcal{B} \uparrow_{\vec{p}^l, \vec{p}^u}^{S,n})$. Let Δ be a Delaunay triangulation of P' . Then, for an appropriately chosen θ , we have $\vec{y} = \theta \cdot P'$. Let $L_y = \theta \cdot L \uparrow^{S,n}(P')$, and $U_y = \theta \cdot U \uparrow^{S,n}(P')$. We need to prove that for any Δ , $L_y \leq f \uparrow^{S,n}(\vec{y}) \leq U_y$. We consider the validity of the lower bound, as the reasoning for the upper bound is symmetric.

Suppose a Δ exists where $L_y \not\leq f \uparrow^{S,n}(\vec{y})$. Define \vec{x} to be the restriction of \vec{y} to $\text{dom}(\mathcal{B})$. A similar restriction of the previous inequality yields $L_{\vec{x}} \not\leq f(\vec{x})$. However, the theorem states that \mathcal{B} encloses f , which is true iff $L_{\vec{x}} \leq f(\vec{x})$. This presents a contradiction. \square

Lifting is one way to extend a bounding set. Another way is to add additional vertices to the bounding set. Unfortunately,

adding vertices does not always preserve function enclosure. However, it is preserved in the special case where the point set is a grid, and the additional vertices are added in such a way that the result remains a grid.

Definition 11 (Grid). *A grid of dimension n is the Cartesian product of n finite subsets of \mathbb{R} , each of which has at least two elements. Given a grid G , we write G_i to refer to the projection of G onto dimension i , so that $G = G_1 \times \dots \times G_n$. The domain of the grid is defined as $\text{dom}(G) = \text{conv}(G)$. The resolution vector $R(G) \in \mathbb{N}^n$ encodes the size of G in each dimension, that is, $R(G)_i = |G_i|$ for each $i \in [1..n]$. If $\vec{g} \in G$ is a point in the grid, then the star of \vec{g} , $S_G(\vec{g})$ is $\{\vec{p} \in G \mid \vec{p}_i = \vec{g}_i \text{ for some } i \in [1..n]\}$.*

For the rest of the paper, we assume that every point set P appearing in a bounding set is a grid.

Definition 12 (Grid Expansion). *Let G be an n -dimensional grid, and let $\vec{q} \in \text{dom}(G)$. Let G'_i be the set $G_i \cup \{q_i\}$. Then G expanded by \vec{q} , written $G + \vec{q}$, is the grid $G'_1 \times \dots \times G'_n$.*

Notice that $G + \vec{q} \setminus G = S_{G'}(\vec{q})$.

Definition 13 (Interpolated Function). *Let $P \subset \mathbb{R}^n$ be a grid, $f : P \rightarrow \mathbb{R}$ a function on P , and Δ a Delaunay triangulation of P . Let $\vec{q} \in \text{dom}(P)$, and let $P' = P + \vec{q}$. Then, f interpolated by \vec{q} using Δ , written $f +_{\Delta} \vec{q}$ is the function $f' : P' \rightarrow \mathbb{R}$ defined as:*

$$(f +_{\Delta} \vec{q})(\vec{x}) = \begin{cases} \theta_{\Delta}(\vec{x}) \cdot f(\text{vect}(S_{\Delta}(\vec{x}))) & \text{if } \vec{x} \in S_G(\vec{q}), \text{ and} \\ f(\vec{x}) & \text{otherwise.} \end{cases}$$

Example 6. *Let \mathcal{B}^1 be the bounding set from Example 1, and let Δ be the triangulation of P_1 whose 2-simplices are the triangles T_1 , with vertices $\vec{p}_1, \vec{p}_2, \vec{p}_3$, and T_2 , with vertices $\vec{p}_2, \vec{p}_3, \vec{p}_4$. Let $\vec{q} = (0, 0)$, and let $P'_1 = P_1 + \vec{q} = P_1 \cup \{(-5, 0), (0, 0), (5, 0), (0, -5), (0, 5)\}$. Then, let $U'_1 = U_1 +_{\Delta} \vec{q}$. Let $\vec{x} = (-5, 0)$. To compute $U'_1(\vec{x})$, we first note that $S_{\Delta}(\vec{x}) = T_1$, $\text{vect}(T_1) = \{\vec{p}_1, \vec{p}_2, \vec{p}_3\}$, and $\theta(\vec{x}) = (0.5, 0.5, 0)$. Thus, $U'_1(\vec{x}) = \theta(\vec{x}) \cdot U_1(\text{vect}(T_1)) = (0.5, 0.5, 0) \cdot (5, 5, 5) = 5$.*

Definition 14 (Interpolated Bounding Set). *Let $\mathcal{B} = \langle n, P, L, U \rangle$ be a bounding set, let Δ be a Delaunay triangulation of P , and let $\vec{q} \in \text{dom}(P)$. Then \mathcal{B} interpolated by \vec{q} using Δ , written $\mathcal{B} +_{\Delta} \vec{q}$, is defined as:*

$$\mathcal{B} +_{\Delta} \vec{q} = \langle n, P + \vec{q}, L +_{\Delta} \vec{q}, U +_{\Delta} \vec{q} \rangle.$$

Example 7. *Let \mathcal{B}^1 be the bounding set from Example 1, Δ the triangulation from Example 6, and $\vec{q} = (0, 0)$. Then $\mathcal{B}^1 +_{\Delta} \vec{q} = \langle 2, P'_1, L_1 +_{\Delta} \vec{q}, U'_1 \rangle$, where P'_1 and U'_1 are as in Example 6, and $L_1 +_{\Delta} \vec{q}$ is computed similarly.*

Theorem 2. *Let $\mathcal{B} = \langle n, P, L, U \rangle$ be a bounding set. If \mathcal{B} encloses a function f , then for every Delaunay triangulation Δ of P and every point $\vec{q} \in \text{dom}(\mathcal{B})$, $\mathcal{B} +_{\Delta} \vec{q}$ also encloses f .*

Proof. Let \vec{q} be an arbitrary point in $\text{dom}(P)$, let $\mathcal{B}' = \mathcal{B} +_{\Delta} \vec{q} = \mathcal{B}' = \langle n, P', L', U' \rangle$, and let Δ' be a Delaunay

triangulation of P' . To show that \mathcal{B}' encloses f , we must show that $(\vec{x}, f(\vec{x})) \in \mathcal{E}(\mathcal{B}', \Delta')$ for every $\vec{x} \in \text{dom}(\mathcal{B}')$. Let $\mathcal{S} = \mathcal{S}_{\Delta'}(\vec{x})$, $V = \text{vert}(\mathcal{S})$, and $\theta = \theta_{\Delta'}(\vec{x})$. Let $L_{\vec{x}} = \theta \cdot L'(V_s)$, and $U_{\vec{x}} = \theta \cdot U'(V_s)$. We consider two cases.

First, we consider the case when the simplex \mathcal{S} is also in a Delaunay triangulation of P . Recall that $\mathcal{B}_{\mathcal{S}}$ is the restriction of the bounding set \mathcal{B} to the simplex \mathcal{S} , obtained by restricting P to only the points in V_s . The restriction of \mathcal{B}' to \mathcal{S} is going to be just the same as the restriction of \mathcal{B} to \mathcal{S} , that is, $\mathcal{B}_{\mathcal{S}} = \mathcal{B}'_{\mathcal{S}}$. So, by substitution, $(\vec{x}, f(\vec{x})) \in \mathcal{P}(\mathcal{B}_{\mathcal{S}})$ iff $(\vec{x}, f(\vec{x})) \in \mathcal{P}(\mathcal{B}'_{\mathcal{S}})$. But we know that \mathcal{B} encloses f , so we must have $(\vec{x}, f(\vec{x})) \in \mathcal{B}_{\mathcal{S}}$. Therefore, $(\vec{x}, f(\vec{x})) \in \mathcal{B}'_{\mathcal{S}}$, and so $(\vec{x}, f(\vec{x})) \in \mathcal{E}(\mathcal{B}', \Delta')$.

The more interesting case is when the simplex \mathcal{S} is not in a Delaunay triangulation of P . For notational convenience, let $I_{\vec{q}} = S_{P'}(\vec{q})$ be the set of points inserted into P to obtain P' . We first show that V_s must contain some elements $I_{\vec{q}}$. To see this, suppose not, so that $V_s \subseteq P$. From the Delaunay condition, we know that $V_{P'}(C(\mathcal{S})^O) = \emptyset$. But since $P \subseteq P'$, we also have that $V_P(C(\mathcal{S})^O) = \emptyset$, making \mathcal{S} a Delaunay simplex of P . \mathcal{S} is therefore in a Delaunay triangulation of P , contradicting our assumption about \mathcal{S} .

We wish to show that $L_{\vec{x}} \leq f(\vec{x}) \leq U_{\vec{x}}$. We focus on the upper bound since the proof for the lower bound is symmetric. Let $\mathcal{Q} = \{C(\mathcal{S}) \mid \mathcal{S} \text{ is a Delaunay } n\text{-simplex of } P'\}$, and let $V_s = \{w_0 = t, w_1, \dots, w_n\}$, where $t \in I_{\vec{q}}$. Now, assume there exists $C \in \mathcal{Q}$ such that $w_k \in \text{conv}(V_P(C))$ for every $k \in [0..n]$. In other words, there is some n -simplex of P whose corresponding circumscribing hypersphere has vertices whose convex hull encloses *all* the points in V_s . This may seem like a strong assumption, but as we show later, such a C always exists. Let $V = V_P(C)$. We define \mathcal{P}_c as the convex hull of $U(V)$, the upper bounding function over V .

The point $U_{\vec{x}}$ is defined as the convex combination of $U'(w_0, w_1, \dots, w_n)$. For every $w_i \in V$, $U'(w_i)$ is the same as $U(w_i)$, guaranteeing containment in \mathcal{P}_c . For $w_i \in I_{\vec{q}}$, $U'(w_i)$ is obtained using gridded interpolation. Recall that $w_i \in \text{conv}(V)$, meaning, $w_i = \theta_v \cdot \text{vert}(\mathcal{S}_v)$, where \mathcal{S}_v is a simplex in a Delaunay triangulation of V , and θ_v is a convex combination variable. Then from the definition of function interpolation, we have $U'(w_i) = \theta_v \cdot U(\text{vert}(\mathcal{S}_v))$. Since $\text{vert}(\mathcal{S}_v) \subseteq V$, $U'(w_i)$ is the convex combination of points in \mathcal{P}_v . From the convexity of \mathcal{P}_v , we have $U'(w_i) \in \mathcal{P}_v$. This ensures that $U'(V_s) \subset \mathcal{P}_c$.

If w_i can be represented as $w_i = \theta_{\phi} \cdot \text{vert}(\phi)$ for some other simplex ϕ , where $\text{vert}(\phi) \not\subseteq V$, then we also have $U'(w_i) = \theta_{\phi} \cdot U(\phi)$. We claim that $\theta_{\phi} \cdot U(\text{vert}(\phi)) = \theta_v \cdot U(\text{vert}(\mathcal{S}_v))$. To see this, note that this case can only arise when w_i is on a face shared by ϕ and some simplex in the triangulation of V (otherwise $w_i \notin \text{conv}(V)$). Since w_i is on the face of a simplex, it is on a k -simplex, where $k < n$. This follows from the property that every face of a simplicial n -complex is a k -simplex, where $k < n$. This means that the only points that determine the value of w_i are the points in $V_k = V \cap \text{vert}(\phi)$. We can rewrite $\text{vert}(\phi)$ as $(V_k \circ V_{\phi})$, where $V_{\phi} = \text{vert}(\phi) \setminus V_k$. Similarly, we can rewrite $\text{vert}(\mathcal{S}_v)$ as $(V_k \circ V_v)$, where $V_v = \text{vert}(\mathcal{S}_v) \setminus V_k$. Since w_i is fully determined by V_k , we can rewrite $w_i = \theta_{\phi} \cdot \text{vert}(\phi)$ as $w_i = (\theta_k \circ \vec{0}) \cdot (V_k \circ V_{\phi})$. Similarly,

we can rewrite $w_i = \theta_v \cdot \text{vert}(\mathcal{S}_v)$ as $w_i = (\theta_k \circ \vec{0}) \cdot (V_k \circ V_v)$. Extending this process to the bounds yields $(\theta_k \circ \vec{0}) \cdot U(V_k \circ V_{\phi})$ and $(\theta_k \circ \vec{0}) \cdot U(V_k \circ V_v)$. Simplifying this expression yields $\theta_k \cdot U(V_k)$ and $\theta_k \cdot U(V_k)$, proving our claim.

Next, we claim that $f(\vec{x}) \leq U_{\vec{x}}^c$, where $U_{\vec{x}}^c$ is the value of the lower face of \mathcal{P}_c at \vec{x} . To see this, note that f being enclosed by \mathcal{B} means that for any $\{v_0, \dots, v_n\} \subseteq V$, $f(\text{conv}(v_0, \dots, v_n)) \leq \text{conv}(U(v_0, \dots, v_n))$. We have $\vec{x} \in \mathcal{S} \subseteq \text{conv}(V)$, meaning that $f(\vec{x}) \leq U_{\vec{x}}^c$. Since $U'(V_s) \subset \mathcal{P}_c$, we know from convexity that $U_{\vec{x}}^c \leq U_{\vec{x}}$. This proves that $f(\vec{x}) \leq U_{\vec{x}}$. We can follow a similar process to show that $L_{\vec{x}} \leq f(\vec{x})$.

To complete the proof, we need to show that there is always a $C \in \mathcal{Q}$ where $w_k \in \text{conv}(V)$ for every $k \in [0..n]$. Assume there isn't. In other words, let w_i be an arbitrary element of V_s , and define the set $\mathcal{Q}_i = \{D \in \mathcal{Q} \mid w_i \in D\}$. Assume there exists a w_j in $V_s \setminus w_i$ for which there is no $D \in \mathcal{Q}_i$ where $w_j \in D$. Since P is a grid, that means w_j is not in the smallest hyperrectangle containing the 1-star of w_i (henceforth called the 1-hyperrectangle). To see this, recall that \mathcal{Q}_i contains all Delaunay spheres that contain w_i . If w_j is in the 1-hyperrectangle of w_i , then we can always construct a Delaunay sphere $C \in \mathcal{Q}$ (with minimum diameter $\|w_i - w_j\|$) that contains both w_i and w_j , violating our assumption. Since w_j is not in the 1-hyperrectangle of w_i , there exists a $\vec{p} \in P'$ where $\vec{p}_k \in [(w_i)_k, (w_j)_k]$ for some coordinate $k \in [1..n]$. Let $\mathcal{R} = \{\vec{p} \in P' \mid \vec{p}_k \in [(w_i)_k, (w_j)_k] \text{ for any } k \in [1..n]\}$. If $V_s = \{w_0, \dots, w_{n-2}, w_i, w_j\}$, then the smallest Delaunay sphere that contains V_s has a minimum diameter of $\|w_i - w_j\|$. By definition, there has to be at least one point in $\mathcal{R} \cap C_s^O$. This is because we can always pick a point \vec{p} in the 1-star of w_i that lies along an arbitrary coordinate projection of the vector formed by $w_i - w_j$. Since there's no construction where C_s has an empty interior, we cannot form a viable Delaunay simplex where there isn't a $C \in \mathcal{Q}$ such that $w_k \in \text{conv}(V)$ for every $k \in [0..n]$. Meaning we can say $f(\vec{x}) \leq U_{\vec{x}}^c \leq U_{\vec{x}}$ in every Delaunay triangulation of P' . \square

We are now ready to consider composing bounding sets. Let $\mathcal{B}^{f'}$ and $\mathcal{B}^{g'}$ be bounding sets and suppose that $\mathcal{B}^{f'}$ encloses f and $\mathcal{B}^{g'}$ encloses g . We want to define $\mathcal{B}^{f'} \bowtie \mathcal{B}^{g'}$ in such a way that it encloses $f \bowtie g$. The first step is to use lifting and interpolation to obtain bounding sets for (lifted versions of) f and g with the *same domain*.

Let $n \in \mathbb{N}$, and let $S^f, S^g \subseteq [1..n]$ such that $[n] = S^f \cup S^g$, $n^f = |S^f|$, and $n^g = |S^g|$. Let $\mathcal{B}^{f'} = \langle n^f, P^f, L^f, U^f \rangle$, and $\mathcal{B}^{g'} = \langle n^g, P^g, L^g, U^g \rangle$. We also assume that $f : \mathbb{R}^{n^f} \rightarrow \mathbb{R}$, and $g : \mathbb{R}^{n^g} \rightarrow \mathbb{R}$.

First, we define $(f \uparrow^{S^f, n})$ and $(g \uparrow^{S^g, n})$ as the lifted versions of f and g . We also define $\mathcal{B}^{f'} \uparrow_{\vec{p}^l, \vec{p}^u}^{S^f, n}$ and $\mathcal{B}^{g'} \uparrow_{\vec{p}^l, \vec{p}^u}^{S^g, n}$ where $\vec{p}^l = \min_i(P)$, and $\vec{p}^u = \max_i(P)$. Theorem 1 ensures that the resulting bounding sets enclose $(f \uparrow^{S^f, n})$ and $(g \uparrow^{S^g, n})$. Next, we ensure that both bounding sets are defined over the same set of points. We achieve this by defining $\mathcal{B}^{f'} \uparrow_{\Delta} P_g$ as the result of inserting every point \vec{p} in P_g into $\mathcal{B}^{f'}$ via gridded interpolation. We define $\mathcal{B}^{g'} \uparrow_{\Delta} P_f$ in a similar fashion. The

resulting bounding sets, \mathcal{B}^f and \mathcal{B}^g are defined over the same point set.

Definition 15 (Bounding Set Composition). *Let $\mathcal{B}^f = \langle n, P, L^f, U^f \rangle$ and $\mathcal{B}^g = \langle n, P, L^g, U^g \rangle$ be bounding sets with the same dimension and over the same set of points P . For $\bowtie \in \{+, -, \times, /\}$, we define $\mathcal{B}^f \bowtie \mathcal{B}^g := \langle n, P, L^{fg}, U^{fg} \rangle$, where, for all $\vec{x} \in P$,*

$$L^{fg}(\vec{x}), U^{fg}(\vec{x}) = \begin{cases} L^f(\vec{x}) + L^g(\vec{x}), U^f(\vec{x}) + U^g(\vec{x}) & \text{if } \bowtie = +, \\ L^f(\vec{x}) - L^g(\vec{x}), U^f(\vec{x}) - U^g(\vec{x}) & \text{if } \bowtie = -, \\ \min(\text{Bounds}), \max(\text{Bounds}) & \text{if } \bowtie \in \{\times, \div\}, \end{cases}$$

where $\text{Bounds} = \{h_1(x) \bowtie h_2(x) \mid h_1 \in \{L^f, U^f\}, h_2 \in \{L^g, U^g\}\}$ is the set of potential bounds when using multiplication or division.

Theorem 3. *Let $\mathcal{B}^f = \langle n, P, L^f, U^f \rangle$ and $\mathcal{B}^g = \langle n, P, L^g, U^g \rangle$ be bounding sets with the same dimension and over the same set of points P . Then, for $\bowtie \in \{+, -, \times, /\}$, $\mathcal{B}^f \bowtie \mathcal{B}^g$ encloses $f \bowtie g$.*

Proof. Let $\mathcal{B}^{fg} = \mathcal{B}^f \bowtie \mathcal{B}^g$, let $x \in \text{dom}(\mathcal{B}^{fg})$ and let Δ be a triangulation of P . Let S be the n -simplex in Δ containing \vec{x} . We must show that $f(\vec{x}) \bowtie g(\vec{x}) \in \mathcal{B}_S^{fg}$.

Let V be a vector containing the points in $\text{vert}(S)$. Then, we can write $\vec{x} = \theta \cdot V$ for some convex combination vector θ . Let $L_{\vec{x}}^{fg} = \theta \cdot L^{fg}(V)$ and $U_{\vec{x}}^{fg} = \theta \cdot U^{fg}(V)$. Showing $f(\vec{x}) \bowtie g(\vec{x}) \in \mathcal{B}_S^{fg}$ reduces to showing $L_{\vec{x}}^{fg} \leq f(\vec{x}) \bowtie g(\vec{x}) \leq U_{\vec{x}}^{fg}$.

Let $L_{\vec{x}}^f = \theta \cdot L^f(V)$, $U_{\vec{x}}^f = \theta \cdot U^f(V)$, $L_{\vec{x}}^g = \theta \cdot L^g(V)$, and $U_{\vec{x}}^g = \theta \cdot U^g(V)$. We know that $(\vec{x}, f(\vec{x})) \in \mathcal{P}(\mathcal{B}_S^f)$ and $(\vec{x}, g(\vec{x})) \in \mathcal{P}(\mathcal{B}_S^g)$, so we have $L_{\vec{x}}^f \leq f(\vec{x}) \leq U_{\vec{x}}^f$ and $L_{\vec{x}}^g \leq g(\vec{x}) \leq U_{\vec{x}}^g$.

Now, if $\bowtie \in \{+, -\}$, we have $L_{\vec{x}}^{fg} = \theta \cdot L^{fg}(V) = \theta \cdot (L^f(V) \bowtie L^g(V)) = \theta \cdot L^f(V) \bowtie \theta \cdot L^g(V) = L_{\vec{x}}^f \bowtie L_{\vec{x}}^g \leq f(\vec{x}) \bowtie g(\vec{x})$. We can similarly show that $f(\vec{x}) \bowtie g(\vec{x}) \leq U_{\vec{x}}^{fg}$.

The situation becomes more complex if $\bowtie \in \{\times, \div\}$. The complexity arises from $\min(h_1(V) \bowtie h_2(V))$ being a pointwise minimization, and from the possibility of division by zero. Let $h_1 \in \{L^f, U^f\}$, and $h_2 \in \{L^g, U^g\}$. For each $v \in V$, we define $h'_1(v)$ and $h'_2(v)$ as $\arg \min(h_1(v) \bowtie h_2(v))$. By definition, we have $h'_1(v) \bowtie h'_2(v) \leq f(v) \bowtie g(v)$. To see this, note that $L^f(v) \bowtie \alpha \leq f(v) \bowtie \alpha$ for any $\alpha \in \mathbb{R}_{>0}$. Similarly, $U^f(v) \bowtie \beta \leq f(v) \bowtie \beta$ for any $\beta \in \mathbb{R}_{<0}$. Therefore $\min(L^f(v) \bowtie \gamma, U^f(v) \bowtie \gamma) \leq f(v) \bowtie \gamma$ for any $\gamma \in \mathbb{R} \setminus 0$. If we assume that $g(v) \in [L^g(v), U^g(v)] \subset \mathbb{R}$, and that $0 \notin [L^g(v), U^g(v)]$, then $\min(L^f(v) \bowtie g(v), U^f(v) \bowtie g(v)) \leq f(v) \bowtie g(v)$. Since $L^g(v) \leq g(v)$, we have $\min(L^f(v) \bowtie L^g(v), U^f(v) \bowtie L^g(v)) \leq f(v) \bowtie g(v)$. Therefore, by definition, we have $h'_1(v) \bowtie h'_2(v) \leq f(v) \bowtie g(v)$. The first assumption holds from \mathcal{B}^g enclosing g . The second assumption is only required to avoid division by zero when $\bowtie = \div$. Since we only consider Lipschitz functions, and therefore can never divide by zero, the second assumption always holds when $\bowtie = \div$. If we remove the second assumption, it is easy to see that the argument still holds when $\bowtie = \times$.

Let $\text{sign}(f(x)|y)$ return $\text{sgn}(y) \cdot f(x)$. By definition, we have $h'_1(v) \leq \min(\text{sign}(L^f(v)|g(v)), \text{sign}(U^f(v)|g(v)))$. In other words, $h'_1(V) \preceq \{\min(\text{sign}(L^f(v)|g(v)), \text{sign}(U^f(v)|g(v))) \mid v \in V\} \preceq f(V)$.

This result, coupled with \mathcal{B}^f enclosing f ensures $\theta \cdot h'_1(V) \leq \min(\text{sign}(L_{\vec{x}}^f|g(x)), \text{sign}(U_{\vec{x}}^f|g(x))) \leq f(x)$. The first inequality follows from the result shown in the preceding paragraph. In other words, if $A \preceq B$, and θ is a convex combination vector (i.e. a sequence of non-negative scalars), then $\theta \cdot A \leq \theta \cdot B$. The second inequality follows from \mathcal{B}^f enclosing f . Likewise, $\theta \cdot h'_2(V) \leq \min(\text{sign}(L_{\vec{x}}^g|f(x)), \text{sign}(U_{\vec{x}}^g|f(x))) \leq g(x)$ follows from a similar argument.

From \mathcal{B}^f enclosing f , we have $L_{\vec{x}}^f \leq f(x) \leq U_{\vec{x}}^f$. For any $\gamma \in \mathbb{R} \setminus 0$, we have $\min(L_{\vec{x}}^f \bowtie \gamma, U_{\vec{x}}^f \bowtie \gamma) \leq f(x) \bowtie \gamma$. Building on the preceding paragraph, we have $\theta \cdot h'_1(V) \bowtie \gamma \leq \min(L_{\vec{x}}^f \bowtie \gamma, U_{\vec{x}}^f \bowtie \gamma)$, therefore, we must also have $\theta \cdot h'_1(V) \bowtie \gamma \leq f(x) \bowtie \gamma$. Since $g(x) \in \mathbb{R} \setminus 0$, we can substitute $g(x)$ for γ to yield $\theta \cdot h'_1(V) \bowtie g(x) \leq f(x) \bowtie g(x)$. However, we know $\theta \cdot h'_2(V) \leq g(x)$ (from the previous paragraph), therefore, $\theta \cdot h'_1(V) \bowtie \theta \cdot h'_2(V) \leq f(x) \bowtie g(x)$. Since $L_{\vec{x}}^{fg} = \theta \cdot L^{fg}(V) = \theta \cdot h'_1(V) \bowtie \theta \cdot h'_2(V)$, we can say $L_{\vec{x}}^{fg} \leq f(x) \bowtie g(x)$. We can use a similar argument to show that $f(x) \bowtie g(x) \leq U_{\vec{x}}^{fg}$. \square

Figure 1 illustrates the effect of applying these operations to our running example.

V. THE OVERTPOLY ALGORITHM

In this section, we present *OvertPoly*, a combinatorial algorithm for verifying nonlinear neural feedback systems. Given a discrete-time neural feedback system \mathcal{D} , the OvertPoly algorithm computes an overapproximation $\hat{\tau}^{\mathcal{D}}(I)$ of the system trajectory $\tau^{\mathcal{D}}(I)$ such that $\tau^{\mathcal{D}}(I)_t \subseteq \hat{\tau}^{\mathcal{D}}(I)_t$ for every $t \in [0, T]$. It verifies safety by checking if $\hat{\tau}^{\mathcal{D}}(I)$ satisfies a specified reach-avoid property. By definition, \mathcal{D} is safe if $\hat{\tau}^{\mathcal{D}}(I)$ is safe. At each time step t , we compute polyhedral enclosures that bound each transition function f_i in F . These enclosures, along with the neural network controller u , are encoded as mixed-integer linear programs (MILPs). To compute $\text{next}^{\mathcal{D}}(\vec{x})_i$ at time step t , the MILP corresponding to each state variable $i \in [1, n]$ is optimized (maximized and minimized) to yield an overapproximation of $\text{next}^{\mathcal{D}}(\vec{x})_i$.

In the following sections, we provide details about each step of the process. Section V-A provides details about how the theory of polyhedral enclosures is used to compute bounds for extended rational nonlinear functions. Section V-B describes an efficient combinatorial representation for polyhedral enclosures. Section V-C discusses how we handle neural network controllers, and Section V-D describes the procedure for computing $\text{next}^{\mathcal{D}}(\vec{x})_i$.

A. Computing Tight Enclosures for Nonlinear Dynamics

Each polyhedral enclosure is computed over a convex domain \mathcal{X}_t . At the start of the verification problem (i.e. $t = 0$), we have $\mathcal{X}_0 \subseteq I$. We assume that \mathcal{X}_t is a hyperrectangle defined as $[l_1, u_1] \times \dots \times [l_n, u_n] \subseteq \mathbb{R}^n$, where each interval $[l_i, u_i]$ is the domain of the i -th component of the state vector

\vec{x} . For each $f_i \in F$, we would like to compute a bounding set \mathcal{B}^i that encloses f_i over the domain \mathcal{X}_t . The Bound algorithm provides an overview of the process for computing \mathcal{B}^i . The inputs to this algorithm are a syntax tree T for the function f_i and the hyperrectangle \mathcal{X}_t . The output is a *polyhedral enclosure* \mathcal{B}^i for the function f_i .

We assume the syntax tree T is constructed such that its leaf nodes represent functions of a single variable. We also assume that each node $v \in T$ stores two objects: A function g , that represents the expression defined by the subtree rooted at v , and an operator \bowtie , representing how the children of v are composed to yield to g . The Bound algorithm computes a polyhedral enclosure for f_i by performing a bottom-up traversal of T . At the leaf nodes, it computes polyhedral enclosures for univariate functions following the process described in Section IV-A. As it travels up the tree, it uses methods based on the theory developed in Section IV-B to compute multivariate polyhedral enclosures from univariate polyhedral enclosures. The result is a polyhedral enclosure for f_i . We repeat this process for every $f_i \in F$.

Function Bound(T, \mathcal{X}_t)

Data: A tree T , a domain \mathcal{X}_t

Result: A polyhedral enclosure \mathcal{B}_i^f for the function represented by T over the input domain \mathcal{X}

```

if  $T.f$  is a constant  $c$  then
  | return  $\langle n, \mathcal{X}_t, c, c \rangle$ 
end
if  $T.f$  is univariate in variable  $\vec{x}_i$  then
  | return  $OvertMod(T.f, l_i, u_i)$  /* univariate
  | enclosure */
end
for  $i = 1 : |T|$  do
  |  $\mathcal{B}^i \leftarrow \text{Bound}(T[i], \mathcal{X}_t)$  /* Bottom up tree
  | traversal */
end
 $\mathcal{B} \leftarrow \mathcal{B}^i$ 
for  $i = 2 : |T| - 1$  do
  | if  $T.op \in \{+, -, \times, \div\}$  then
  | |  $\mathcal{B} \leftarrow \text{Compose}(\mathcal{B}, \mathcal{B}^i, T.op)$  /* resolve
  | | subtrees */
  | else
  | | return error /* Unsupported operator
  | | */
  | end
end
return  $\mathcal{E}$ 

```

B. Generating an Efficient Optimization Model for the Enclosures

Computing $next^{\mathcal{D}}(\vec{x})_i$ requires an efficient combinatorial representation of each polyhedral enclosure (\mathcal{B}^i) generated in Section V-A. To this end, we employ the aggregated convex combination method [15]. Let $d = |P^i|$ (i.e. the number of points in P^i , where P^i is the point set for the over which \mathcal{B}^i is defined). Let Δ be a Delaunay triangulation of P^i , with

$m = |\Delta|$ denoting the number of simplices in Δ . We would like to represent an arbitrary $\vec{x} \in \mathcal{X}_t$ as the convex combination of some simplex $S \in \Delta$.

We begin by defining a sequence of binary variables (b_1, \dots, b_m) to encode the *active* simplex in Δ . In other words, if $x \in S_k$, then $b_k = 1$, and $b_i = 0$ for every $i \in [1..m] \setminus k$. We define λ as a convex combination variable. Unlike the convex combination variables we've used thus far, λ is not defined with respect to a simplex. Instead, it is defined over all points in P^i (i.e. $\lambda \in \mathbb{R}^d$). We use \vec{p} to denote points in P^i . Using these variables, we can define an integer program \mathcal{M}_i for \mathcal{B}^i .

$$\sum_{j=1}^d \lambda_j = 1, \quad \lambda_j \geq 0, \quad \sum_{i=1}^m b_i \leq 1, \quad b_i \in \{0, 1\}^m \quad (6a)$$

$$\lambda_j \leq \sum_{\{i | \mathbf{p}_j \in \text{vert}(S_i)\}} b_i \quad \text{for } j = 1, \dots, d \quad (6b)$$

$$\mathbf{x} = \sum_{j=1}^d \lambda_j \cdot \mathbf{p}_j \quad (6c)$$

$$\bar{y} = \sum_{j=1}^d \lambda_j \cdot \bar{f}(\mathbf{p}_j), \quad \underline{y} = \sum_{j=1}^d \lambda_j \cdot \underline{f}(\mathbf{p}_j) \quad (6d)$$

$$\underline{y} \leq y \leq \bar{y} \quad (6e)$$

Equation (6a) defines the auxiliary variables of the model (λ and b), and enforces that only one binary variable can be active at a time. Equation (6b) defines the SOS-2 constraint. The SOS-2 constraint requires that only points from simplices adjacent to the active simplex can have nonzero convex combination weights, thereby enforcing continuity. Equation (6c) defines the state variable \vec{x} , while Equation (6d) defines the polyhedral enclosure for state variable \vec{x}_i 's transition function. Finally, Equation (6e) defines the transition function (f_i) as a surface contained within the polyhedral enclosure.

We construct a separate mixed integer program for the enclosure of every transition function f_i in F . This yields a finite set of problems $\{\mathcal{M}_1, \dots, \mathcal{M}_n\}$ representing the transition function of each state variable. Figure 2 illustrates these constraints for the Unicycle example.

C. Generating an exact representation of the neural network controller

We construct an additional integer program \mathcal{M}_0 to represent u , the neural network controller. The construction follows the methods described in Section II-D.

D. Computing forward reachable sets

To compute $\tau^{\mathcal{D}}(\mathcal{X}_0)_T$ (i.e. the system trajectory from time step 0 to time step T), we need to compute $\mathcal{X}_{t+1} = next^{\mathcal{D}}(\mathcal{X}_t)$ for every $t \in [0..T-1]$. We describe the process for computing \mathcal{X}_{t+1} for an arbitrary $t \in [0..T-1]$. We assume wlog that \mathcal{X}_t is known. To compute \mathcal{X}_{t+1} , we need to compute $next^{\mathcal{D}}(\vec{x})$ for every $\vec{x} \in \mathcal{X}_t$. This process is called *forward reachability analysis*. Since we deal with nonlinear systems, an exact computation of \mathcal{X}_{t+1} is intractable. Instead, we

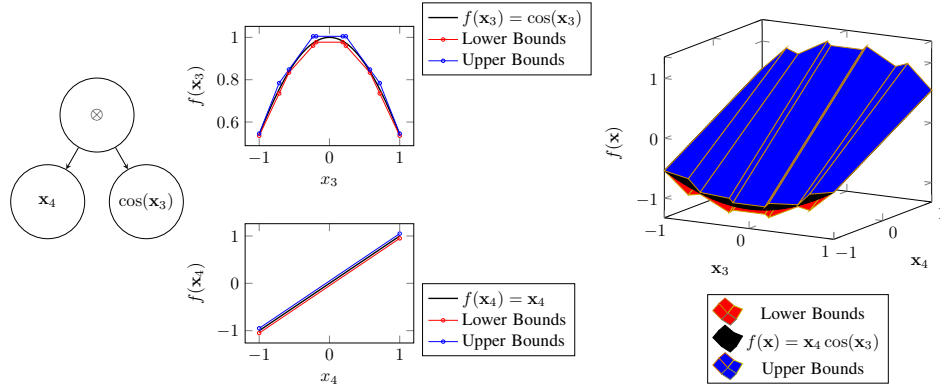


Fig. 1. Overview of bounding algorithm for example problem. We bound $\cos(\mathbf{x}_3)$ and \mathbf{x}_4 , yielding a polyhedral enclosure with (exaggerated) vertices $[(-1.0, -1.051, -0.949) (1.0, 0.949, 1.051)]$, and $[(-1.0, 0.535, 0.546) (-0.716, 0.734, 0.785) (-0.576, 0.833, 0.849) (-0.233, 0.96, 1.005) (-0.189, 0.977, 1.005) (0.189, 0.977, 1.005) (0.233, 0.96, 1.005) (0.576, 0.833, 0.849) (0.716, 0.734, 0.785) (1.0, 0.535, 0.546)]$. We multiply these enclosures to obtain the polyhedral enclosure with vertices $[(-1.0, -1.0, -0.54) (-0.716, -1.0, -0.896) (-0.576, -1.0, -0.856) (-0.233, -1.0, -1.102) (-0.189, -1.0, -1.053) (0.189, -1.0, -1.053) (0.233, -1.0, -1.102) (0.576, -1.0, -0.856) (0.716, -1.0, -0.896) (1.0, -1.0, -0.54) (-1.0, 1.0, 0.541) (-0.716, 1.0, 0.584) (-0.576, 1.0, 0.821) (-0.233, 1.0, 0.83) (-0.189, 1.0, 0.912) (0.189, 1.0, 0.912) (0.233, 1.0, 0.83) (0.576, 1.0, 0.821) (0.716, 1.0, 0.584) (1.0, 1.0, 0.541)]$

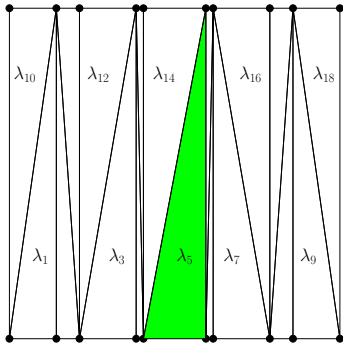


Fig. 2. A visualization of Equations 6a – 6b for a lower dimensional projection of our running example. Equation (6c) is implicitly defined here as well because \vec{x} is the union of these points.

focus on computing an overapproximation $\hat{\mathcal{X}}_{t+1}$ such that $\mathcal{X}_{t+1} \subseteq \hat{\mathcal{X}}_{t+1}$. To do this, we replace the nonlinear transition functions (F) with bounds formed by polyhedral enclosures. Since we have enclosures \mathcal{B}_t^i for every $f_i \in F$, we can construct piecewise linear upper and lower bounds for f_i such that $\forall \vec{x} \in \mathcal{X}_t, \underline{f}_i(\vec{x}) \leq f_i(\vec{x}) \leq \overline{f}_i(\vec{x})$. In other words, we can replace $f_i(\vec{x})$ with the piecewise linear functions $\underline{f}_i(\vec{x})$, and $\overline{f}_i(\vec{x})$ to solve the following problems for every $i \in [1..n]$.

$$\min_{\vec{x} \in \hat{\mathcal{X}}_t} \vec{x}_i + (\underline{f}_i(\vec{x}) + u(\vec{x})_i + \epsilon) \cdot \delta \quad (7a)$$

$$u(\vec{x}) = \mathcal{M}_0(\vec{x}) \quad (7b)$$

$$\epsilon \in E \quad (7c)$$

$$\max_{\vec{x} \in \hat{\mathcal{X}}_t} \vec{x}_i + (\overline{f}_i(\vec{x}) + u(\vec{x})_i + \epsilon) \cdot \delta \quad (7d)$$

$$u(\vec{x}) = \mathcal{M}_0(\vec{x}) \quad (7e)$$

$$\epsilon \in E \quad (7f)$$

Since $\underline{f}_i(\vec{x}) \leq f_i(\vec{x}) \leq \overline{f}_i(\vec{x})$, then solving the problems in eq. (7) for every $i \in [n]$ yields interval bounds $[l'_i, u'_i]$

such that we can define $\hat{\mathcal{X}}_{t+1} = [l'_1, u'_1] \times \dots \times [l'_n, u'_n]$. Constructing $\hat{\tau}^{\mathcal{D}}(I)$ sequentially by repeating this process for each $t \in [0..T-1]$ is called *concrete reachability analysis* [38].

This approach to constructing $\hat{\tau}^{\mathcal{D}}(I)$ has a crucial limitation. Since $\mathcal{X}_{t+1} \subseteq \hat{\mathcal{X}}_{t+1}$, some error $\mathcal{O}_{t+1} = \hat{\mathcal{X}}_{t+1} \setminus \mathcal{X}_{t+1}$ is introduced with each application of eq. (7). Therefore, sequential application of eq. (7) may lead to a large \mathcal{O}_T , a situation referred to as *excess conservatism*. Instead of sequentially solving eq. (7), we could solve the following recursive problem

$$\min_{\vec{x} \in \hat{\mathcal{X}}_t} \vec{x}_i + (\underline{f}_i(\vec{x}) + u(\vec{x})_i + \epsilon) \cdot \delta \quad (8a)$$

$$u(\vec{x}) = \mathcal{M}_0(\vec{x}) \quad (8b)$$

$$\epsilon \in E \quad (8c)$$

$$\hat{\mathcal{X}}_t = \text{next}^{\mathcal{D}}(\hat{\mathcal{X}}_{t-1}) \quad (8d)$$

$$\max_{\vec{x} \in \hat{\mathcal{X}}_t} \vec{x}_i + (\overline{f}_i(\vec{x}) + u(\vec{x})_i + \epsilon) \cdot \delta \quad (8e)$$

$$u(\vec{x}) = \mathcal{M}_0(\vec{x}) \quad (8f)$$

$$\epsilon \in E \quad (8g)$$

$$\hat{\mathcal{X}}_t = \text{next}^{\mathcal{D}}(\hat{\mathcal{X}}_{t-1}) \quad (8h)$$

Constructing $\hat{\tau}^{\mathcal{D}}(I)$ by solving the recursive problem in eq. (8) is called *symbolic reachability analysis* [38]. However, solving eq. (8) presents some challenges. Each transition function $f_i \in F$ may depend on a subset of the entire previous state $\vec{x} \in \mathcal{X}_t$. This dependency induces a *dependency graph*. A dependency graph $G = (V, E)$ encodes dependence relationships between the state variables of each transition function. The model representing state variable \vec{x}_i is assigned a vertex $\mathcal{M}_i \in V$. The neural network controller u is also assigned a vertex $\mathcal{M}_0 \in V$. Two vertices $v_i, v_j \in V$ share an edge if the transition function corresponding to v_i depends on v_j or vice versa. Note that we treat the neural network

controller as the transition function for the control variable u . Figure 3 illustrates the state dependency graph for our running example

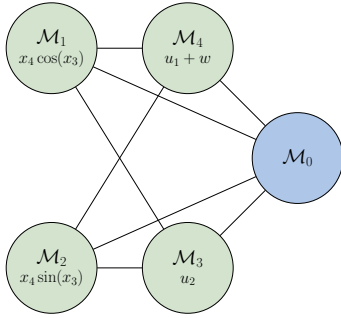


Fig. 3. Dependency graph for Unicycle example. The green vertices represent state variables, while the blue vertex represents the neural network controller. Note that each variable is connected to the controller because the neural network depends on the full state.

The key challenge with solving the recursive problem in eq. (8) is that at each time step t , the transition function $f_i \in F$ depends not only on a subset of the entire previous state \mathcal{X}_t , but also on a subset of every state in $(\mathcal{X}_0, \dots, \mathcal{X}_t)$. Since we compute a polyhedral enclosure for each f_i over the domain \mathcal{X}_t , at each time step t , we need to encode the dependency relationship between the polyhedral enclosures at each time step. We call this relationship a temporal dependency. In other words, if $((\mathcal{M}_0^0, \mathcal{M}_1^0, \dots, \mathcal{M}_n^0), \dots, (\mathcal{M}_0^t, \mathcal{M}_1^t, \dots, \mathcal{M}_n^t))$ represents the models generated by applying the methods from Sections V-A to V-C to each state in $(\hat{\mathcal{X}}_0, \dots, \hat{\mathcal{X}}_t)$, then we need to encode $\hat{\mathcal{X}}_{t+1} = \text{next}^{\mathcal{D}}(\hat{\mathcal{X}}_t)$ for each $t \in [0..t-1]$. Figure 4 illustrates the variable dependency graph induced by the combination of state and temporal dependency in our running example.

The OvertPoly algorithm computes forward reachable sets by solving the integer linear programs in eqs. (7) and (8). It uses the variable dependency graph structure to encode state dependency in the case of concrete reachability, and state/temporal dependency in the case of symbolic reachability.

VI. IMPLEMENTATION

We exploit the meta-programming features of the Julia programming language for expression parsing and symbolic analysis. We use the Symbolics.jl [16] package for analytical derivatives, IntervalRootfinding.jl [23] for sound root finding, and OVERT.jl [38] for univariate bound computation. We combine methods from OVERTVerify.jl and NeuralVerification.jl [30] for our local implementation of MIPVerify. We use the Plasmio framework [21], [22] to solve MILPs on graphs, with Gurobi as a backend solver [17].

VII. EVALUATION

A. Other tools

We evaluate the performance of our tool by comparing it to a discrete-time implementation of CORA [26], a state-of-the-art propagation based tool, and OVERTVerify [38], a state-of-the-art combinatorial tool. We use the Polynomial Zonotope

Function OvertPoly(G, s)

Data: A graph $G = (V, E)$ encoding the dependency graph induced by the trajectory $(\hat{\mathcal{X}}_0, \dots, \hat{\mathcal{X}}_t)$ of a neural feedback system \mathcal{D} up to time t , a binary variable $s \in \{0, 1\}$ indicating whether we wish to compute a concrete or symbolic reachable set

Result: A hyperrectangle $\hat{\mathcal{X}}_{t+1}$ representing an overapproximation of the forward reachable set $\text{next}^{\mathcal{D}}(\hat{\mathcal{X}}_t)$

for $\mathcal{M}_i^t \in V$ **do**

$$l_i = \min_{\vec{x} \in \hat{\mathcal{X}}_t} \vec{x}_i + (\underline{f}_i(\vec{x}) + u(\vec{x})_i + \epsilon) \cdot \delta$$

s.t.:

$$\underline{f}_i(\vec{x}) = \mathcal{M}_i^t(\vec{x}), u(\vec{x}) = \mathcal{M}_0^t(\vec{x}), \epsilon \in E,$$

$$s \cdot \hat{\mathcal{X}}_t = s \cdot \text{next}^{\mathcal{D}}(\hat{\mathcal{X}}_{t-1})$$

$$u_i = \max_{\vec{x} \in \hat{\mathcal{X}}_t} \vec{x}_i + (\overline{f}_i(\vec{x}) + u(\vec{x})_i + \epsilon) \cdot \delta$$

s.t.:

$$\overline{f}_i(\vec{x}) = \mathcal{M}_i^t(\vec{x}), u(\vec{x}) = \mathcal{M}_0^t(\vec{x}), \epsilon \in E,$$

$$s \cdot \hat{\mathcal{X}}_t = s \cdot \text{next}^{\mathcal{D}}(\hat{\mathcal{X}}_{t-1})$$

end

return $[l_1, u_1] \times \dots \times [l_n, u_n]$

abstraction [26] in CORA. We note that the performance of the CORA algorithm depends on the choice of hyper-parameters, and we report results for the lowest-precision settings needed to verify a given property. Since our approach is based on the OVERT algorithm, we maintain the same hyperparameters when comparing our algorithm to OVERTVerify.

B. Benchmarks

We test our algorithm on a subset of the benchmarks used in the annual ARCH-Competition [31]. Since we only support ReLU networks, we restrict ourselves to benchmarks that use ReLU networks. We describe pertinent details about these benchmarks in the following sections.

1) *Single Pendulum*: We would like to verify that the angle of an inverted pendulum remains within a specified range during a specified time interval. Formally, we define the neural feedback system \mathcal{P} , where $n^{\mathcal{P}} = 2$, $I^{\mathcal{P}} = [1.0, 1.2] \times [0.0, 0.2]$, $F^{\mathcal{P}}(\vec{x}) = (\vec{x}_2, c_1 \vec{x}_1 - c_2 \vec{x}_2)$, $E^{\mathcal{P}} = \{0\} \times \{0\}$, $u^{\mathcal{P}}$ is computed by a neural network with two hidden layers (each with 25 neurons), and two outputs, the first of which is set to the constant zero value, $\delta^{\mathcal{P}} = 0.05$, $T^{\mathcal{P}} = 20$, and $G^{\mathcal{P}} = \emptyset$. Let R be the set defined by $[0, 1] \times [-\infty, \infty]$, then $A^{\mathcal{P}}$ is the sequence of sets defined by

$$A^{\mathcal{P}}(t) = \begin{cases} \emptyset, & \text{if } t < 10 \\ R^c & \text{if } 10 \leq t \leq 20 \end{cases}$$

We would like to verify that Equation (5) holds for \mathcal{P} .

2) *ACC*: In this benchmark, we would like to verify that a neural network controlled vehicle tracks a set velocity while maintaining a safe distance from a second vehicle. Formally, we define the neural feedback system \mathcal{A} , where $n^{\mathcal{A}} = 6$, $I^{\mathcal{A}} = [90, 110] \times [32, 32.2] \times \{0\} \times [10, 11] \times [30, 30.2] \times \{0\}$,

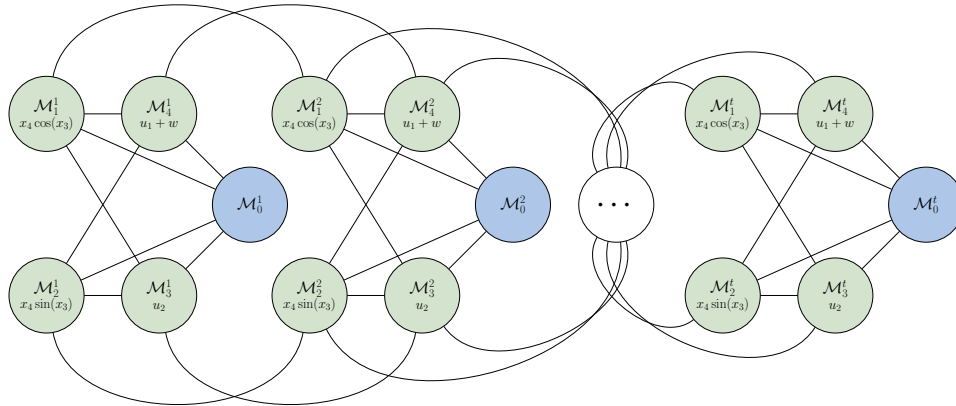


Fig. 4. Symbolic dependency graph for the Unicycle car model. The state dependency graphs are identical at each time step (since the transition functions are time invariant), but there are edges connecting models across time steps.

	OvertPoly		OVERTVerify		CORA	
	Time (s)	Volume	Time (s)	Volume	Time (s)	Volume
Single Pendulum	1.6431	5.533E-2	1.9232	5.53E-2	2.919	7.6388
ACC	23.1960	3.819E-3	345.0036	1.119E-2	25.4478	6.1596E+5
TORA	1461.5640	6.434E-1	13620.0628	6.434E-1	×	6.0325e + 02
Unicycle	7217.153	8.979E-6	40109.9396	9.865E-6	×	×

TABLE I

BENCHMARK COMPUTATION TIME (S) AND SET VOLUMES. COMPUTATION TIMES LISTED FOR VERIFIED INSTANCES, AND × FOR UNVERIFIED INSTANCES. ALL AVAILABLE SET VOLUMES LISTED. BEST PERFORMANCE IS HIGHLIGHTED IN BOLD.

$F^A(\vec{x}) = (\vec{x}_2, \vec{x}_3, -2\vec{x}_3 - c_1\vec{x}_2^2, \vec{x}_5, \vec{x}_6, -2\vec{x}_6 - c_1\vec{x}_5^2), E^A = \{0\} \times \{0\} \times \{0\} \times \{0\}$, u^A is computed by a neural network with five hidden layers (each with 20 neurons), and six outputs, of which outputs 1,2,4, and 5 are set to the constant zero value, and output 3 is set to the constant -4 value, $\delta^A = 0.1$, $T^A = 50$, and $G^A = \emptyset$. Let R be the set of states satisfying $\vec{x}_1 - \vec{x}_4 \geq 10 + 1.4 \cdot \vec{x}_5$ then A^A is the sequence of sets defined by

$$A^A(t) = \begin{cases} R^c, & \text{if } 0 \leq t \leq 50 \\ \emptyset & \text{if } t > 50 \end{cases}$$

We would like to verify that Equation (5) holds for \mathcal{A} .

3) *TORA*: We would like to verify that the states of an actuated cart remain within a safe region during a specified time interval. Formally, we define the neural feedback system \mathcal{T} , where $n^T = 4$, $I^T = [0.6, 0.7] \times [-0.7, -0.6] \times [-0.4, -0.3] \times [0.5, 0.6]$, $F^T(\vec{x}) = (\vec{x}_2, -\vec{x}_1 + 0.1 \sin(\vec{x}_3), \vec{x}_4, 0)$, $E^T = \{0\} \times \{0\} \times \{0\} \times \{0\}$, u^T is computed by a neural network with three hidden layers (each with 100 neurons), and four outputs, the first three of which is set to the constant zero value, $\delta^T = 0.1$, $T^T = 20$, and $G^T = \emptyset$. Let R be the set defined by $[-2, 2] \times [-2, 2] \times [-2, 2] \times [-2, 2]$, then A^P is the sequence of sets defined by

$$A^P(t) = \begin{cases} R^c, & \text{if } 0 \leq t \leq 20 \\ \emptyset & \text{if } t > 20 \end{cases}$$

We would like to verify that Equation (5) holds for \mathcal{T} .

4) *Unicycle Car Model*: See Section III-A

C. Hardware

Computation times for the Pendulum, ACC, and TORA are obtained by running all tools on 16 Intel i9-9980HK CPU cores @ 2.40GHz. The Unicycle benchmark is harder to verify, and we obtain results by running OVERTVerify and OVERTPoly on a computer with 16 Intel XEON E5-2637 CPU cores.

D. Results

The performance of our tool is compared to the state of the art in Table I. For each benchmark, we evaluate each tool on the amount of time required to verify (or falsify) the specified property, as well as the volume of the reachable set at time T . Since the CORA algorithm does not support volume computation for polynomial zonotopes, we convert the final set into an interval, and evaluate the volume of the interval. Despite employing a combinatorial approach, our computation time is comparable to state of the art propagation-based methods.

1) *Single Pendulum*:: The Single Pendulum benchmark was used as a baseline for all tools. OvertPoly and OVERTVerify are able to falsify the property in less than 2 seconds. Despite using the lowest precision setting, CORA required around 3 seconds to falsify the property.

2) *ACC*:: OvertPoly and CORA are able to verify the ACC benchmark in under 30 seconds, while OVERTVerify required around 350 seconds to verify the same property. The discrepancy between the OVERTVerify and OvertPoly sets can be explained by the need to introduce an additional input layer

to the benchmark to make it compatible with the OVERTVerify benchmark.

3) *TORA*:: CORA is unable to verify the TORA benchmark. We tried all available hyperparameter combinations, but the set generated by CORA was too large to verify the property. OvertPoly and OVERTVerify are both able to verify the property. OvertPoly is able to verify the property an order of magnitude faster than OVERTVerify.

4) *Unicycle*:: CORA is similarly unable to verify the Unicycle benchmark (the tool crashes due to state explosion), while OvertPoly and OVERTVerify require a combination of concrete and symbolic approaches to verify the property. OvertPoly is able to verify the property around 5 times faster than OVERTVerify.

Symbolic reachability is the most precise algorithm for computing forward reachable sets of nonlinear discrete time neural feedback systems. This precision comes at the cost of computational tractability. The computational intractability of symbolic reachability makes it an ideal test of the scalability of combinatorial algorithms. Figure 5 highlights the scaling differences between OvertPoly and OVERTVerify.

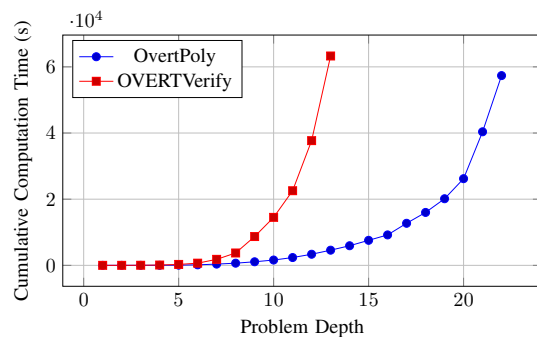


Fig. 5. Pure symbolic reachability comparison between OverPoly and OVERTVerify using the Unicycle benchmark. Each tool was used to compute as many pure symbolic reachable steps as possible with a (per optimizer call) timeout of 3600 seconds.

The figure shows an order of magnitude scaling improvement over OVERTVerify. As we consider longer horizon symbolic problems, OvertPoly appears to scale better than OVERTVerify. On our running example, OvertPoly is able to solve a 13-step symbolic problem an order of magnitude faster than OVERTVerify.

VIII. CONCLUSIONS

In this manuscript, we showed that polyhedral enclosures are a scalable abstraction for verifying reach-avoid properties for nonlinear neural feedback systems. Polyhedral enclosures (along with neural network controllers) are encoded as mixed integer linear programs, enable forward reachability analysis of discrete time systems. This is the essence of the OvertPoly algorithm, which showed an order of magnitude improvement in computation time/precision over comparable tools. The improved scalability of precise verification tools should enable the verification of more realistic neural feedback systems, thereby ensuring safer transportation systems

REFERENCES

- [1] Althoff, M.: Reachability analysis of nonlinear systems using conservative polynomialization and non-convex sets. In: Proceedings of the 16th international conference on Hybrid systems: computation and control. pp. 173–182 (2013)
- [2] Althoff, M., Kochdumper, N.: Cora 2016 manual. TU Munich **85748** (2016)
- [3] Althoff, M., Stursberg, O., Buss, M.: Reachability analysis of nonlinear systems with uncertain parameters using conservative linearization. In: 2008 47th IEEE Conference on Decision and Control. pp. 4042–4048. IEEE (2008)
- [4] Bansal, S., Chen, M., Herbert, S., Tomlin, C.J.: Hamilton-jacobi reachability: A brief overview and recent advances. In: 2017 IEEE 56th Annual Conference on Decision and Control (CDC). pp. 2242–2253. IEEE (2017)
- [5] Bogomolov, S., Forets, M., Frehse, G., Potomkin, K., Schilling, C.: Juliareach: a toolbox for set-based reachability. In: Proceedings of the 22nd ACM International Conference on Hybrid Systems: Computation and Control. pp. 39–44 (2019)
- [6] Boyd, S., Vandenberghe, L.: Convex optimization. Cambridge university press (2004)
- [7] Chen, X., Abrahám, E., Sankaranarayanan, S.: Flow*: An analyzer for non-linear hybrid systems. In: Computer Aided Verification: 25th International Conference, CAV 2013, Saint Petersburg, Russia, July 13–19, 2013. Proceedings 25. pp. 258–263. Springer (2013)
- [8] Duong, T., Altawaitan, A., Stanley, J., Atanasov, N.: Port-hamiltonian neural ode networks on lie groups for robot dynamics learning and control. arXiv preprint arXiv:2401.09520 (2024)
- [9] Dutta, S., Chen, X., Sankaranarayanan, S.: Reachability analysis for neural feedback systems using regressive polynomial rule inference. In: Proceedings of the 22nd ACM International Conference on Hybrid Systems: Computation and Control. pp. 157–168 (2019)
- [10] Eittinger, S., Cheng, S., Caine, B., Liu, C., Zhao, H., Pradhan, S., Chai, Y., Sapp, B., Qi, C.R., Zhou, Y., et al.: Large scale interactive motion forecasting for autonomous driving: The waymo open motion dataset. In: Proceedings of the IEEE/CVF International Conference on Computer Vision. pp. 9710–9719 (2021)
- [11] Everett, M.: Neural network verification in control. In: 2021 60th IEEE Conference on Decision and Control (CDC). pp. 6326–6340. IEEE (2021)
- [12] Everett, M., Habibi, G., How, J.P.: Robustness analysis of neural networks via efficient partitioning with applications in control systems. IEEE Control Systems Letters **5**(6), 2114–2119 (2021). <https://doi.org/10.1109/LCSYS.2020.3045323>
- [13] Everett, M., Habibi, G., Sun, C., How, J.P.: Reachability analysis of neural feedback loops. IEEE Access **9**, 163938–163953 (2021)
- [14] Fan, J., Huang, C., Chen, X., Li, W., Zhu, Q.: Reachnn*: A tool for reachability analysis of neural-network controlled systems. In: International Symposium on Automated Technology for Verification and Analysis. pp. 537–542. Springer (2020)
- [15] Geißler, B., Martin, A., Morsi, A., Schewe, L.: Using piecewise linear functions for solving minlps. In: Mixed integer nonlinear programming, pp. 287–314. Springer (2011)
- [16] Gowda, S., Ma, Y., Cheli, A., Gwózdź, M., Shah, V.B., Edelman, A., Rackauckas, C.: High-performance symbolic-numeric via multiple dispatch. ACM Commun. Comput. Algebra **55**(3), 92–96 (jan 2022). <https://doi.org/10.1145/3511528.3511535>
- [17] Gurobi Optimization, LLC: Gurobi Optimizer Reference Manual (2024), <https://www.gurobi.com>
- [18] Huang, C., Fan, J., Chen, X., Li, W., Zhu, Q.: Polar: A polynomial arithmetic framework for verifying neural-network controlled systems. In: International Symposium on Automated Technology for Verification and Analysis. pp. 414–430. Springer (2022)
- [19] Ivanov, R., Carpenter, T.J., Weimer, J., Alur, R., Pappas, G.J., Lee, I.: Verifying the safety of autonomous systems with neural network controllers. ACM Transactions on Embedded Computing Systems (TECS) **20**(1), 1–26 (2020)
- [20] Ivanov, R., Weimer, J., Alur, R., Pappas, G.J., Lee, I.: Verisig: verifying safety properties of hybrid systems with neural network controllers. In: Proceedings of the 22nd ACM International Conference on Hybrid Systems: Computation and Control. pp. 169–178 (2019)
- [21] Jalving, J., Cao, Y., Zavala, V.M.: Graph-based modeling and simulation of complex systems. Computers & Chemical Engineering **125**, 134–154 (2019)

- [22] Jalving, J., Shin, S., Zavala, V.M.: A graph-based modeling abstraction for optimization: concepts and implementation in Plasmol. *Mathematical Programming Computation* **14**, 699–747 (2022). <https://doi.org/10.1007/s12532-022-00223-3>
- [23] JuliaIntervals: Intervalrootfinding.jl. <https://github.com/JuliaIntervals/IntervalRootFinding.jl> (2024), accessed: 2024-11-18
- [24] Kaufmann, E., Bauersfeld, L., Loquercio, A., Müller, M., Koltun, V., Scaramuzza, D.: Champion-level drone racing using deep reinforcement learning. *Nature* **620**(7976), 982–987 (2023)
- [25] Kochdumper, N., Althoff, M.: Sparse polynomial zonotopes: A novel set representation for reachability analysis. *IEEE Transactions on Automatic Control* **66**(9), 4043–4058 (2020)
- [26] Kochdumper, N., Althoff, M.: Constrained polynomial zonotopes. *Acta Informatica* pp. 1–38 (2023)
- [27] Kochdumper, N., Schilling, C., Althoff, M., Bak, S.: Open-and closed-loop neural network verification using polynomial zonotopes. In: *NASA Formal Methods Symposium*. pp. 16–36. Springer (2023)
- [28] Kurková, V.: Kolmogorov’s theorem is relevant. *Neural computation* **3**(4), 617–622 (1991)
- [29] Ladner, T., Althoff, M.: Automatic abstraction refinement in neural network verification using sensitivity analysis. In: *Proceedings of the 26th ACM International Conference on Hybrid Systems: Computation and Control*. pp. 1–13 (2023)
- [30] Liu, C., Armon, T., Lazarus, C., Strong, C., Barrett, C., Kochenderfer, M.J.: Algorithms for verifying deep neural networks (2020), <https://arxiv.org/abs/1903.06758>
- [31] Lopez, D.M., Althoff, M., Forets, M., Johnson, T.T., Ladner, T., Schilling, C.: Arch-comp23 category report: Artificial intelligence and neural network control systems (ainncs) for continuous and hybrid systems plants. In: *EPiC Series in Computing* (2023)
- [32] Lopez, D.M., Choi, S.W., Tran, H.D., Johnson, T.T.: Nnv 2.0: the neural network verification tool. In: *International Conference on Computer Aided Verification*. pp. 397–412. Springer (2023)
- [33] Lutterkort, D., Peters, J.: Optimized refinable enclosures of multivariate polynomial pieces. *Computer Aided Geometric Design* **18**(9), 851–863 (2001). [https://doi.org/https://doi.org/10.1016/S0167-8396\(01\)00067-X](https://doi.org/https://doi.org/10.1016/S0167-8396(01)00067-X), <https://www.sciencedirect.com/science/article/pii/S016783960100067X>
- [34] Muller, J.M., Muller, J.M.: *Elementary functions*. Springer (2006)
- [35] Peters, J., Wu, X.: On the optimality of piecewise linear max-norm enclosures based on slfes. In: *International Conference on Curves and Surfaces*, Saint-Malo, France. Citeseer (2002)
- [36] Rober, N., Everett, M., Zhang, S., How, J.P.: A hybrid partitioning strategy for backward reachability of neural feedback loops. In: *2023 American Control Conference (ACC)*. pp. 3523–3528 (2023). <https://doi.org/10.23919/ACC55779.2023.10156051>
- [37] Schilling, C., Forets, M., Guadalupe, S.: Verification of neural-network control systems by integrating Taylor models and zonotopes. In: *AAAI*. pp. 8169–8177. AAAI Press (2022). <https://doi.org/10.1609/aaai.v36i7.20790>, <https://ojs.aaai.org/index.php/AAAI/article/view/20790>
- [38] Sidrane, C., Maleki, A., Irfan, A., Kochenderfer, M.J.: Overt: An algorithm for safety verification of neural network control policies for nonlinear systems. *Journal of Machine Learning Research* **23**(117), 1–45 (2022)
- [39] Siefert, J.A., Bird, T.J., Koeln, J.P., Jain, N., Pangborn, H.C.: Successor sets of discrete-time nonlinear systems using hybrid zonotopes. In: *2023 American Control Conference (ACC)*. pp. 1383–1389. IEEE (2023)
- [40] Tjeng, V., Xiao, K., Tedrake, R.: Evaluating robustness of neural networks with mixed integer programming. *arXiv preprint arXiv:1711.07356* (2017)
- [41] Tomlin, C.J., Mitchell, I., BAYEN, A.M., Oishi, M.: Computational techniques for the verification of hybrid systems. *Proceedings of the IEEE* **91**(7), 986–1001 (2003)
- [42] Tordesillas, J., How, J.P.: Minvo basis: Finding simplexes with minimum volume enclosing polynomial curves. *Computer-Aided Design* **151**, 103341 (2022)
- [43] Vincent, J.A., Schwager, M.: Reachable polyhedral marching (rpm): A safety verification algorithm for robotic systems with deep neural network components. In: *2021 IEEE International Conference on Robotics and Automation (ICRA)*. pp. 9029–9035. IEEE (2021)
- [44] Wang, Y., Zhou, W., Fan, J., Wang, Z., Li, J., Chen, X., Huang, C., Li, W., Zhu, Q.: Polar-express: Efficient and precise formal reachability analysis of neural-network controlled systems. *IEEE Transactions on Computer-Aided Design of Integrated Circuits and Systems* (2023)
- [45] Zhang, Y., Xu, X.: Reachability analysis and safety verification of neural feedback systems via hybrid zonotopes. In: *2023 American Control Conference (ACC)*. pp. 1915–1921. IEEE (2023)
- [46] Ziegler, G.M.: *Lectures on polytopes*, vol. 152. Springer Science & Business Media (2012)